Host-cell interactions and innate immune response to an enteric pathogen in a human intestinal enteroid-neutrophil co-culture

Jose M. Lemme-Dumit,[1] Michele Doucet,[2] Nicholas C. Zachos,[2]* Marcela F. Pasetti[1]*

[1]Department of Pediatrics, Center for Vaccine Development and Global Health, University of Maryland School of Medicine, Baltimore, MD, USA.

[2]Department of Medicine, Division of Gastroenterology and Hepatology, Johns Hopkins University School of Medicine, Baltimore, MD, USA.

*Corresponding authors:

Marcela F. Pasetti, Ph.D.
685 West Baltimore St.; HSF-I Room 480
Baltimore, MD 21201
Email: mpasetti@som.umaryland.edu
Phone: 410-706-2341; Fax: 410-706-6205

Nicholas C. Zachos, Ph.D.
720 Rutland Avenue; Ross Research Building Room 943
Baltimore, MD 21205
Email: nzachos1@jhmi.edu
Phone: 410-614-0128; Fax: 410-955-9677

Abstract

Polymorphonuclear neutrophils (PMN) respond to inflammation and infection in the gut. The physical and molecular interactions between the human intestinal epithelium and PMN in the gut mucosa and their coordinated responses to enteric pathogens, are poorly understood. We have established a PMN-enteroid co-culture model consisting of human intestinal stem-cell derived enteroid monolayers and peripheral blood PMN. The model was characterized in terms of tissue structure, barrier function, cell phenotype, production of cytokines, and innate immune responses. *Shigella* was used as a model enteric pathogen to interrogate PMN and epithelial cell interactions and innate immunity. PMN added to the enteroid monolayers increased production of IL-8 and rapidly transmigrated across the epithelial cell layer. PMN immune phenotype was distinctly modified in the gut microenvironment via molecular signals and direct epithelial cell contact. Apical exposure to *Shigella* increased PMN migration and production of IL-6 by co-cultured cells. PMN became activated and efficiently phagocytosed bacteria at the apical epithelial cell surface. The co-culture model revealed PMN-epithelial cell direct communication, tissue-driven PMN phenotypic adaptation and enhancement of anti-microbial function. This novel *ex vivo* epithelial cell-PMN co-culture system is relevant for mechanistic interrogation of host-microbe interactions and innate immune responses and the evaluation of preventive/therapeutic tools.

Introduction

The intestinal epithelium creates a physical and molecular barrier that protects the host from potentially damaging elements in the constantly changing outside environment. Epithelial barrier function is supported by a diverse population of underlying immune cells, which deploy a variety of host-defense mechanisms against harmful agents.[1] Coordinated signals resulting from microbial sensing, cell-to-cell contact, cytokines, and other chemical mediators determine the type and extent of responses of immune cells in the gut mucosa, balancing tissue homeostasis with effective anti-microbial function via inflammation.

Advances in understanding intestinal physiology, pathophysiology, and host immunity have traditionally relied on studies conducted in animal models (or animal tissue) and in traditional tissue culture systems using colon cancer cell lines. Animal models, including the use of mutant mouse strains, have contributed to the mechanistic understanding of the composition, function, regulatory processes, and operatives of immunity at the gut mucosa. Unfortunately, host restrictions limit the utility and value of animal models.[2, 3] This is the case for many enteric pathogens for which small animals fail to recreate disease as it occurs in humans. Likewise, immortalized (transformed) cell lines (e.g. HT-29, Caco-2, and T84) do not reflect human physiological responses but the behavior of aberrant diseased cells (e.g. karyotype defects). These cell-line based cultures also lack the multicellular complexity of the human intestinal epithelium, which further reduces the reliability and significance of the data generated.

The establishment of human enteroids from $Lgr5^{+}$ intestinal stem cells was a breakthrough in tissue culture technology.[4] Since then, three-dimensional (3D) intestinal enteroids have been widely used as models to study human gut physiology and pathophysiology as well as host-microbe interactions.[5-7] Not only do enteroids render a truer physiological representation of the human epithelium, but they also offer a practical and reliable system to probe mechanisms and interventions at the gut mucosal interface. The 3D spheroid conformation can be adapted to produce a 2D monolayer configuration with enteroids seeded on a semipermeable membrane

(i.e. Transwell insert).[8-10] An important practical advantage to this simplified format is that it allows for direct and controlled access to the apical (mimicking the lumen) and basolateral side of the epithelial cells, thus facilitating experimental manipulation and evaluation of outcomes. These enteroid monolayers, which can be generated from any gut segment, reproduce the undifferentiated (crypt-like) and differentiated (villus-like) profile of the intestinal epithelial cells (i.e. absorptive enterocytes, goblet cells, enteroendocrine cells, and Paneth cells) and display segment-specific phenotypic and functional attributes of the normal human gut.[11] To better recreate the cellular complexity of the gastrointestinal mucosal barrier, we devised a co-culture consisting of enteroid monolayers and human primary macrophages on the basolateral side.[12, 13] The enteroid-macrophage co-culture model allowed us to demonstrate physical and cytokine/chemokine-mediated interactions between intestinal epithelial cells and macrophages in the presence of pathogenic *E. coli*. Aiming to improve and expand this model to examine the role of other phagocytic cells in gut mucosal immunity, we herein report the establishment of an *ex vivo* co-culture model containing intestinal epithelial cells and human primary polymorphonuclear neutrophils (PMN) facing the monolayers' basolateral side. This co-culture model was characterized by analysis of histology, PMN phenotype, PMN-epithelial cell physical and molecular interactions and cell function. Coordinated epithelial and PMN anti-microbial response was examined using *Shigella* as model enteric pathogen. *Shigella* causes diarrhea and dysentery in humans by trespassing the colonic barrier via M cells and infecting epithelial cells, and this process involves massive recruitment of PMN.[14] The enteroid-PMN co-culture modeled the paradoxical role of PMN contributing to inflammation and controlling infection.

Results

Establishment of a PMN-enteroid co-culture and PMN-epithelial cell interaction. To model PMN function in the human gut, we established an enteroid-PMN co-culture model that contains human enteroid monolayers and freshly isolated human PMN. The configuration of this model is

similar to that of the human enteroid-macrophage co-culture developed by our group.[12, 13] Human ileal 3D organoids derived from $Lgr5^+$-containing biopsies from healthy subjects were seeded upon the inner (upper) surface of a Transwell insert and allowed to grow until they reached confluency. PMN isolated from peripheral blood of healthy human adult volunteers, exhibiting a $CD15^+CD16^+CD14^-$ phenotype were seeded on the outer (bottom) surface of the insert (Fig. 1a).[15] Confocal immunofluorescence microscopy and H&E staining of the PMN-enteroid co-cultures confirmed the expected epithelial cell polarity with the brush border oriented towards the luminal side (apical compartment) and adherent PMN facing the basolateral side of the monolayer (Fig. 1b). A striking observation was the rapid mobilization of PMN from the bottom side of the insert (where they were seeded) towards the epithelium. Within 2h of being added to the monolayers, PMN migrated from the insert and through the insert's pores, and intercalated within the epithelial cells (Fig. 1b, c). Further, PMN crossed through the epithelial monolayer and erupted on the apical surface (Fig. 1c). The process created a hole in the otherwise confluent epithelium. The migrating PMN could be enumerated in the apical compartment media (Fig. 1d). The addition of PMN increased membrane permeability, shown as decrease in transepithelial electrical resistance (TER), although the difference did not reach statistical significance (Fig. 1e).

Since cell movement is influenced by molecular mediators, we next examined the presence of cytokines (pro- and anti-inflammatory) and chemoattractant molecules in media collected from the apical and basolateral compartments of enteroid monolayers alone and enteroid-PMN co-cultures. Basolateral levels of IL-8 were 10-fold higher in the enteroid-PMN co-cultures (Fig. 1f), while MCP-1 and TNF-α remained unaffected. The presence of PMN did not affect apical secretion of MCP-1, IL-8 and TNF-α (Fig. 1f). Production of MCP-1 was distinctly polarized, with higher levels being released to the apical side. IL-1β, IL-6, IL-10, IL-12p70, IFN-γ, and TGF-β1 were measured but found to be non-detectable.

Because human IL-8 promotes PMN migration,[16] we examined the effect of exogenous IL-8 on the co-cultured PMN and on monolayer permeability. Apical treatment of monolayers with 100 ng/ml rhIL-8 increased PMN migration (1.8-fold) (Fig. 1g) and barrier permeability; the previously observed PMN-induced decrease in TER became statistically significant in the presence of IL-8 (Fig. 1h). IL-8 alone did not affect the permeability of monolayers. Taken together, these results demonstrate adequate engraftment of PMN on the basolateral side of the enteroid monolayer, rapid migration of PMN across the monolayer (moving to the luminal side), PMN-induced basolateral secretion of IL-8, and membrane de-stabilization (increased permeability) by IL-8-enhanced PMN transepithelial movement.

The human intestinal epithelium environment determines PMN immune phenotype and functional capacity. Cell phenotype, morphology, and function can be affected by the surrounding tissue and molecular environment. We hypothesized that the immune phenotype and functional capacity of PMN added to the enteroid monolayer would be influenced by their proximity or direct contact with the intestinal epithelium. To explore this hypothesis, we investigated the expression of cell surface markers and phenotypic features of PMN freshly isolated from peripheral blood in comparison with those of PMN in the enteroid co-culture; two populations of co-cultured PMN were investigated following 2h of incubation: PMN harvested from the basolateral media (tissue adjacent milieu) or PMN residing within the monolayer and in direct contact with the epithelial cells (Fig. 2a). PMN co-cultured with enteroid monolayers had a distinct phenotypic profile as compared with peripheral blood PMN. Regardless of the location, PMN co-cultured with enteroid monolayers exhibited increased expression of CD18 (β2 integrin), a molecule that participates in extravasation of circulating PMN, and CD47, a receptor for membrane integrins involved in cell adhesion and migration (Fig. 2b). In contrast, the expression of CD182 (CXCR2 or IL-8RB) was reduced in co-culture PMN (Fig. 2b). CD66b, a marker of secondary granule exocytosis and CD88 (C5a receptor), a molecule that mediates chemotaxis,

granule enzyme release, and super anion production were likewise increased, although only in PMN in the basolateral media (not in contact with cells) (Fig. 2c). PMN in close contact with epithelial cells exhibited increased expression of CD15 (E-selectin), which mediates PMN extravasation; CD16 (FcγRIII), a receptor for IgG that mediates degranulation, phagocytosis, and oxidative burst; and CD11b (α integrin), a protein that facilitates PMN adhesion and, along with CD18, forms the Mac-1 complex implicated in multiple anti-microbial functions (e.g. phagocytosis, cell-mediated cytotoxicity, cellular activation) (Fig. 2d). These results demonstrate unique phenotypic adaptations of PMN within the intestinal epithelial environment, some of which were driven by molecular signals while others required direct PMN-epithelial cell contact.

PMN interaction with *Shigella* as a model enteric pathogen. To study PMN and epithelial cell interactions in the context of an enteric infection, we used wild type *Shigella flexneri* 2a (strain 2457T) as a model pathogen. PMN participate in *Shigella* pathogenesis through secretion of pro-inflammatory cytokines and deploy anti-microbial functions including phagocytosis, proteolytic enzymes, anti-microbial proteins, and neutrophil extracellular trap (NET) production. We first determined baseline responses of PMN exposed to *Shigella*. PMN phagocytosed FITC-labeled wild-type *S. flexneri* 2a within 10 min of exposure; bacterial uptake increased over time (up to 1h) reaching a maximum effect at 30 min (Fig. 3a). In parallel, the number of bacteria in the culture supernatant of PMN-*Shigella* decreased significantly within 30- and 60-min exposure, in comparison to culture supernatant of *Shigella* alone, in the absence of PMN (Fig. 3b). The proportion of viable PMN was not affected during the first 2h, but decreased significantly 3h post infection (Fig. 3c). *Shigella*-exposed PMN exhibited changes in cell morphology and motility; formation of pseudopodia (projections of the cell membrane that enables locomotion) was observed within 30 min post infection (Fig. 3d). PMN displayed dynamic amoeboid motility toward the bacteria, and release of NETs (Fig. 3e). FITC-stained *Shigella* colocalized with

148 phagolysosome (Fig. 3f). PMN supernatants 2h post infection revealed increased production and
149 secretion of IL-8 and IL-1β, which are key molecular mediators of *Shigella* pathogenesis, as well
150 as downregulation of IL-6 and MCP-1. TNF-α was not affected (Fig. 3g). IL-10, TGF-β1, and IFN-
151 γ were also measured but were below the limit of assay detection. These results revealed that
152 PMN anti-microbial function against *Shigella* involved morphological changes, phagocytic activity,
153 and modulation of inflammatory cytokines.
154
155 **Cellular and molecular responses to *Shigella* in the PMN-enteroid co-culture model**. We
156 used the human PMN-enteroid co-culture model to interrogate PMN and epithelial cell interactions
157 and coordinated responses to *Shigella*. PMN-enteroid co-cultures were produced as described
158 above (Fig. 1a), allowed to settle for 2h, and then apically exposed to wild type *S. flexneri 2a*
159 (MOI=10) for 2h. Non-exposed co-cultures served as controls. Consistent with our previous
160 observation, PMN facing the basolateral side of the cells moved swiftly through the filter pores,
161 passed through the epithelial cells, and protruded on the apical side of the monolayer. PMN
162 basolateral-apical transmigration increased in the presence of *Shigella* (Fig. 4a). PMN traversing
163 across the monolayer phagocytosed bacteria as evidenced by confocal fluorescent microscopy
164 (Fig. 4b; $CD16^+$ PMN are stained in green, engulfed *S. flexneri* 2a in red; actin in white). Addition
165 of PMN to the enteroid monolayers enabled *Shigella* to reach the basolateral side, whereas alone,
166 *Shigella* was unable to trespass the intact enteroid (Fig. 4c). Reduced (1.3-fold) TER values were
167 observed in the *Shigella*-exposed PMN-co-culture as compared with *Shigella*-exposed
168 monolayers alone (Fig. 4d), consistent with loss of barrier function and tissue damage that allowed
169 bacterial translocation.
170 We next examined cytokines produced by *Shigella*-infected and non-infected PMN-enteroid co-
171 cultures. MCP-1, TNF-α, and IL-8 were detected apically and basolaterally, as described above.
172 *Shigella* infection resulted in reduced production of MCP-1 and TNF-α apically as well as

increased production of IL-6 and substantially reduced secretion of IL-8 basolaterally (Fig. 4e). IL-6 was only detected in infected cultures and exhibited basolateral polarization (Fig. 4e). Cultures were also tested for presence of IL-1β, which along with IL-8, are hallmarks of *Shigella* pathogenesis, but was not detectable. Collectively, these observations demonstrate that *Shigella* infection causes active recruitment of PMN to the luminal side, which results in discernible damage of the enteroid monolayer that enables *Shigella* penetration and basolateral infection; still PMN actively engulfed bacteria and increased production of inflammatory cytokines on the apical and basolateral sides, respectively.

Exposure of PMN-enteroid co-cultures to *Shigella* changes PMN immune phenotype. We next examined phenotypic markers of PMN co-cultured with epithelial cells before and after exposure to *Shigella* by flow cytometry. PMN in the infected co-cultures exhibited increased expression of CD88, CD47, and CD66b as compared with non-infected co-cultures (Fig. 5a). Expression of CD15 and CD18, on the other hand, was decreased on PMN from *Shigella*-infected co-cultures (Fig. 5b). CD16, CD11b, and CD182, remained unchanged (Fig. 5c). These results suggest that PMN residing in the intestinal environment undergo immune phenotypic changes as a result of pathogen exposure consistent with increase anti-microbial function.

Discussion

Epithelial cells and innate phagocytic cells underlying the intestinal epithelium work synergistically preventing the trespassing of harmful agents and deploying rapid and effective host defense mechanisms against pathogens. PMN are the first innate immune cells recruited in response to gastrointestinal tissue inflammation and infection and they play a critical role in innate immune responses.[17] Patients with PMN disorders are prone to recurrent microbial infection.[18, 19] Here, we successfully established an *ex vivo* primary human intestinal epithelial and PMN co-culture and

198 used of this model to interrogate cell interactions and innate responses to *Shigella* as a model
199 enteric pathogen.
200 Our group developed the first *ex vivo* human co-culture of enteroids and monocyte-derived
201 macrophages in a monolayer format.[12, 13] The same approach was used to produce the enteroid-
202 PMN co-culture described herein. Differently from macrophages, which remained in the
203 basolateral side of the monolayer (where seeded) and responded to luminal organisms by
204 extending transepithelial projections between epithelial cells, PMN rapidly migrated from the
205 basolateral side of the epithelial cell and across the monolayer, exiting through the apical surface.
206 Histological and confocal microscopy images revealed PMN crawling through the Transwell insert
207 pores, embedding at the base of the epithelial cells, and bursting off the apical side of the enteroid
208 monolayer, all within a few hours of co-culture. While macrophages contributed to cell
209 differentiation and stabilized the epithelial barrier in our previous studies, the PMN transmigration
210 observed herein resulted in functional increase in barrier permeability that enabled bacteria
211 invasion. Intestinal epithelial repair events (e.g. cell proliferation and migration, and closure of
212 leaking epithelial lateral spaces) reportedly begin minutes after acute mucosal barrier injury.[20] As
213 a corollary of this study, we are investigating tissue healing subsequent to PMN-induced
214 inflammation and cell disruption, and the mechanisms and elements involved.
215 The capacity of PMN to migrate across the vascular endothelium[21] and a variety of tissues[22, 23]
216 and epithelial cell layers[24-27] has been documented *in vivo* (mainly in animal models) or *in vitro*
217 using cell lines. These processes have been associated with PMN activation as a result of
218 microbial sensing, inflammation, or danger signals. The level of myeloperoxidase (MPO) in stool
219 is, in fact, a maker of inflammatory bowel disease severity.[28] In our human primary PMN and
220 intestinal epithelial cells co-culture model, PMN migrated even in the absence of external
221 stimulatory signals. PMN are not typically present in the homeostatic gut (but actively recruited
222 by signs of inflammation or infection);[29] therefore, unprovoked PMN migration would not be
223 expected.

The tissue microenvironment can influence immune cell phenotype and effector function.[30, 31] Our results thus suggest that PMN activation in the co-culture was triggered by tissue-derived signals. PMN from peripheral blood exhibited rapid phenotypic changes when incubated with enteroid monolayers. Compared to the PMN from peripheral blood, PMN co-cultured with epithelial cells had increased expression of CD18, which favors cell binding and CD47, which supports transmigration across endothelial and epithelial cells.[32-34] Their phenotype was also influenced by their specific location, whether they were in direct contact with epithelial cells or simply exposed to basolateral culture media. PMN in close proximity with the enterocytes (the migratory ones) had upregulated expression of CD15, which participates in chemotaxis and extravasation from circulation, as well as FcγRIII (CD16), a low affinity Fc receptor for IgG, and CD11b, a marker of cell adhesion and anti-microbial function (phagocytosis, degranulation, oxidative burst).[35, 36] PMN in the basolateral media, on the other hand, had increased expression of CD66b and C5aR (CD88), indicative of functional activity and typically associated with degranulation and chemotaxis, respectively. This is to our knowledge the first detailed description of dynamic changes of PMN immune phenotype in a translationally relevant model of the human intestinal epithelium.

MCP-1/CCL2, a chemoattractant and enhancer of bacterial killing and survival of phagocytic cells and IL-8, a potent promoter of PMN migration and tissue infiltration,[37, 38] were abundantly produced by the ileal monolayers in our co-culture model. TNF-α, a recruiter and activator of phagocytic cells[39] was also present, albeit at lower levels. IL-8 was further sourced by the PMN added to the co-culture, which likely enhanced PMN transmigration. Likewise, the cytokine profiles revealed differences in macrophage and PMN innate immune function within the co-culture; while macrophages contributed to high levels of IFN-γ and IL-6, these cytokines were not detected in the PMN co-culture. The model was therefore capable of reflecting structural and functional cell adaptation.

Human intestinal enteroids can be infected with *Shigella*.[40, 41] *In vivo*, the bacteria invade the colonic and rectal mucosa and causes severe inflammation, massive recruitment of PMN, and tissue destruction.[14] Bloody/mucous diarrhea (dysentery) with large numbers of PMN in stool are hallmarks shigellosis in humans.[42] Hence *Shigella* infection was fitting to interrogate coordinated innate responses of co-cultured epithelial cells and PMN to an enteric pathogen. *Shigella* added on the luminal surface of the monolayers increased basolateral-apical PMN migration. Early efflux of PMN into the colonic tissue has been observed during shigellosis in the infected rabbit loop model.[43] PMN transmigration has also been reported *in vitro* using colonic T84 cells.[43, 44] Consistent with previous reports, PMN transmigration in our co-culture caused microscopically visible epithelial cell damage and created a conduit for bacterial invasion and possibly amplification of infection. We are currently studying reverse transmigration of bacteria-loaded PMN (out of the lumen and back to the basolateral side) as a possible means to initiate adaptive immunity through cross-presentation.

Although acting in a “brute force” manner, PMN deployed potent anti-microbial activity against *Shigella*. Bacteria incubated with PMN from circulation were phagocytosed within minutes and entrapped in NET structures. These PMN increased production of IL-8 and the pyroptosis-inducer IL-1β, and downregulated IL-6 and MCP-1. Larger numbers of PMN transmigrated to the apical compartment in the *Shigella*-infected co-culture and had robust phagocytic capacity. Intriguingly, IL-8 levels were reduced, IL-1β was absent, and IL-6 was increased in the infected (compared to non-infected) PMN co-culture. A reduction of IL-8 production had been reported in *Shigella*-infected human colonic explants, which was ascribed to anti-inflammatory bacterial proteins or death of IL-8 secreting cells.[45] Reduced levels of these inflammatory cytokines may also reflect a regulatory role to prevent further tissue damage. Heightened levels of IL-6 and reduced TNF-α during infection may suggest a protective epithelial mechanism after injury.[46, 47] In addition, IL-6

has been attributed a beneficial role in enhancing Th17-protective immunity against *Shigella* re-infection.[48]

The immune phenotype of PMN in the co-culture adapted again as a result of *Shigella* infection, with further increases in activation/granule-associated markers CD66b, CD88, and CD47. CD47 has been implicated in PMN paracellular migration through epithelial cells in response to bacterium-derived leukocyte chemoattractant N-formyl-methionyl-leucyl-phenylalanine, in a process that involved intracellular distribution and increased CD47 cell surface expression.[33] CD47-deficient mice have increased susceptibility to *E. coli* as a result of reduced PMN trafficking and bacterial killing activity.[49] This finding is consistent with our observed upregulation of CD47 in *Shigella*-exposed PMN, which is likely associated with PMN's antimicrobial activity. CD16 and CD11b expression were unaltered on PMN co-cultured with intestinal enteroids and exposed to *Shigella*, indicating a preserved phagocytic capacity, whereas extravasation and cell adhesion markers CD15 and CD18 were downregulated. It has been reported that CD47 expression increases gradually and modulates CD11b-integrin function and CD11b/CD18 surface expression on PMN, suggesting a regulatory mechanism between these molecules.[33, 50] Expression of CD47 is self-protective; it avoids clearance by phagocytic cells.[51] The exact role of CD47 expression on PMN during *Shigella* infection remains to be elucidated.

Human intestinal xenografts in immunodeficient mice have been used to model interactions of *Shigella* with the human intestine *in vivo*. The model failed to discern any role of PMN in ameliorating or exacerbating disease, but revealed larger intracellular bacteria in PMN-depleted mice; the authors conclude that while PMN may contribute to tissue damage, they are important in controlling bacteria dissemination. The combination of species, immunodeficient background, and impracticality are major confounders/limitations of this model.[52]

The PMN-epithelial cell co-culture described here provides a translationally relevant *ex vivo* model to study human epithelial cell-PMN physiology and pathophysiology, as well as host cell interactions and innate responses to enteric organisms. Our studies provided new insights on the

close communication between PMN and epithelial cells and their coordinated responses to *Shigella* as a model gastrointestinal pathogen. These studies also contributed new knowledge on the ability of the human gut environment to induce phenotypic and functional changes on recruited PMN. This model could be useful to interrogate innate immune defense mechanisms to enteric pathogens and to support the development and evaluation of preventive or therapeutic tools.

Materials and methods

Human PMN isolation

Human peripheral blood was collected in EDTA tubes (BD Vacutainer) from healthy volunteers enrolled in University of Maryland Institutional Review Board (IRB) approved protocol #HP-40025-CVD4000, and methods were conducted in compliance with approved Environmental Health and Safety guidelines (IBC #00003017). PMN were obtained by Ficoll-Paque (PREMIUM solution, GE Healthcare Bio-Sciences AB, Sweden) gradient centrifugation following dextran (Alfa Aesar, USA) sedimentation.[53] Contaminating erythrocytes were removed by hypotonic lysis. After washing, cells (>95% of PMN determined by flow cytometry and May-Grunwald-Giemsa stained cytopreps) were suspended in enteroid differentiation media (DFM) without antibiotics and immediately used. Cell counting and viability were determined using Guava Viacount Flex Reagent (Luminex, USA) following the manufacturer's instruction and analyzed in Guava 8HT using Viacount software (Luminex, USA).

Tissue collection and enteroid generation

Human enteroid cultures were established from biopsy tissue obtained after endoscopic or surgical resection from healthy subjects at Johns Hopkins University under Johns Hopkins University IRB approved protocol #NA-00038329, as previously described.[54] Briefly, enteroids generated from isolated intestinal crypts from ileal segments were maintained as cysts embedded in Matrigel (Corning, USA) in 24-well plates and cultured in Wnt3A and Rspo-1 containing non-

differentiated media (NDM).[55] Multiple enteroid cultures were harvested with Culturex Organoid Harvesting Solution (Trevigen, USA), and small enteroid fragments were obtained by digestion with TrypLE Express (ThermoFisher) in 37°C water bath for 90 seconds. Enteroid fragments were resuspended in NDM containing 10 μM Y-27632 and 10 μM CHIR 99021 inhibitors (Tocris) (NDM+inhibitors). The inner surface of Transwell inserts (3.0 μm pore transparent polyester membrane) pre-coated with 100 μl of human collagen IV solution (34 μg/ml; Sigma-Aldrich, USA) were seeded with 100 μl of an enteroid fragment suspension, and 600 μl of NDM+inhibitors was added to the wells of the receiver plate and incubated at 37°C, 5% CO_2 as previously described.[55] NDM without inhibitors were replaced after 48h, and fresh NDM was added every other day; under these conditions, enteroid cultures reached confluency in 14-16 days. Monolayer differentiation was induced by incubation in Wnt3A-free and Rspo-1-free DFM without antibiotics for 5 days. Monolayer confluency was monitored by measuring TER values with an epithelial voltohmmeter (EVOM^2; World Precision Instruments, USA). The unit area resistances (ohm*cm^2) were calculated according to the growth surface area of the inserts (0.33 cm^2).

PMN-enteroid co-culture

Differentiated enteroid monolayers seeded on Transwell inserts were inverted and placed into an empty 12-well plate. PMN (5x10^5 in 50 μl of DFM) were added onto the bottom surface of the inserts and cells were allowed to attach for 2h at 37°C, 5% CO_2 (inserts remained wet throughout this process). The inserts were then turned back to their original position into a 24-well receiver plate, and DFM was added to the insert (100 μl) and into the well (600 μl). Approximately 45% of the total PMN remained attached to the Transwell insert. TER measurements were collected after 2h allowing monolayer recovering.

***Shigella flexneri* 2a infection**

Shigella flexneri 2a wild type strain 2457T was grown from frozen stocks (-80°C) on Tryptic Soy Agar (TSA) (Difco BD, USA) supplemented with 0.01% Congo Red dye (Sigma-Aldrich) overnight at 37°C. Bacterial inoculum was made by resuspending single red colonies in sterile 1X PBS pH 7.4 (Quality Biological). Bacterial suspension was adjusted to the desired concentration (~$1x10^8$ CFU/ml) in advanced DMEM/F12 without serum. A bacterial suspension containing ~ $5x10^6$ CFU in 50 μl was added directly to PMN (for 10-60 min) or to the apical compartment of enteroid monolayers alone or enteroid-PMN co-culture (for 2h) a multiplicity of infection of 10 relative to 1 PMN.

PMN transmigration

Basolateral-to-apical PMN transmigration was quantified by measurement of PMN MPO using a commercial kit (Cayman Chemical, Ann Arbor, MI) as previously described.[56] The assay was standardized with a known number of human PMN. MPO activity in lysates of enteroid monolayer alone was negligible.

PMN phagocytosis

S. flexneri 2a cultures grown overnight as described above were washed, resuspended in sterile PBS and incubated with FITC (Sigma-Aldrich) (20 μg/ml) for 30 min at 37ºC. The bacteria suspension was thoroughly washed and adjusted to ~10^8 CFU/ml in sterile PBS/glycerol (1:2), and stored at -80ºC until used. The day of the assay, FITC-labeled *Shigella* was incubated with PMN-autologous human sera for 30 min at 37ºC. Opsonized bacteria $5x10^6$ CFU was added to PMN suspension ($5x10^5$ cells) and incubated for 10, 30, and 60 min. Phagocytosis was measured by flow cytometry. External fluorescence was blocked with the addition of trypan blue, and the difference between MFI blocked and non-blocked samples was used to calculate % phagocytosis.[57, 58]

375

376 **H&E and immunofluorescence staining**

377 PMN-enteroid co-culture cells were fixed in aqueous 4% paraformaldehyde (PFA; Electron
378 Microscopy Sciences, USA) at room temperature (RT) for 45 min and then washed with PBS. For
379 H&E staining, monolayers were kept for at least 48h in formaldehyde solution, then embedded in
380 paraffin, sectioned, mounted on slides, and stained with H&E. For immunofluorescence, cells
381 were permeabilized and blocked for 30 min at RT in PBS containing 15% FBS, 2% BSA, and
382 0.1% saponin (all Sigma-Aldrich, USA). Cells were rinsed with PBS and incubated overnight at
383 4ºC with primary antibodies: mouse anti-CD16 (LSBio, USA), rabbit anti-*S. flexneri* 2a (Abcam,
384 USA) diluted 1:100 in PBS containing 15% FBS and 2% BSA. Stained cells were washed with
385 PBS and incubated with secondary antibodies: goat anti-mouse AF488, goat anti-rabbit AF594
386 (all ThermoFisher, USA) diluted 1:100 in PBS 1h at RT; phalloidin staining was included in this
387 step AF594 or AF633 (Molecular Probes, ThermoFisher) for actin visualization. Cells were
388 washed and mounted in ProLong Gold Antifade Reagent with DAPI (Cell Signaling Technology,
389 USA) for nuclear staining and maintained at 4ºC. Lysosome was stained with LysoTracker™ Red
390 DND-99 (ThermoFischer) following the manufacturer's instructions.

391

392 **Immunofluorescence microscopy**

393 Confocal imaging was carried out at the Confocal Microscopy Facility of the University of Maryland
394 School of Medicine using a Nikon W1 spinning disk confocal microscope running NIS-Elements
395 imaging software (Nikon). Images were captured with a 40X or 60X oil objective and settings were
396 adjusted to optimize signal. Immunofluorescence imaging (Fig. 3f) was carried out using EVOS
397 FL Imaging systems (fluorescent microscope) at 40X objective lens. Images were collated using
398 FIJI/ImageJ (NIH). Signal processing was applied equally across the entire image. Actin channel
399 was arranged to white-grey color for contrast purpose.

400

401 **Flow cytometry**

402 Cell phenotype was determined using the following human specific monoclonal antibodies from
403 BD Pharmingen: HI98 (anti-CD15, FITC-conjugated), M5E2 (anti-CD14, APC-conjugated), 3G8
404 (anti-CD16, PE/Cy7-conjugated), D53-1473 (anti-CD88, BV421-conjugated), and BioLegend:
405 TS1/18 (anti-CD18, PE/Cy7-conjugated), ICRF44 (anti-CD11b, BV421-conjugated), 5E8/CXCR2
406 (anti-CD182, APC-conjugated), CC2C6 (anti-CD47, PE/Cy7-conjugated), HA58 (anti-CD54,
407 APC-conjugated), G10F5 (anti-CD66b, Pacific Blue-conjugated). PMN were blocked with 2%
408 normal mouse serum (ThermoFisher) for 15 min at 4ºC. After washing, cells were resuspended
409 in FACS buffer (PBS containing 0.5% BSA and 2 mM EDTA; all Sigma-Aldrich) and 100 μl of
410 equal number of cells were dispensed in several tubes and stained with antibodies for 30 min at
411 4ºC. Antibodies were used diluted 1:2 – 1:1,000; optional amount was determined by in-house
412 titration. Cells were washed in FACS buffer and either analyzed or fixed in 4% PFA for 15 min at
413 4ºC and analyzed the next day. Marker expression was analyzed in a Guava 8HT using Guava
414 ExpressPro software (Luminex, USA) or BD LSRII using FACSDiva software (BD Biosciences,
415 USA) and analyzed with FlowJo software (v10, Tree Star).
416
417 **Cytokine and chemokine measurements**
418 Cytokines and chemokines were measured by electrochemiluminescence microarray using
419 commercial assays (Meso Scale Diagnostic, USA) following the manufacturer's instructions. IFN-
420 γ, IL-1β, IL-6, IL-10, IL-12p70, TNF-α, MCP-1, TGF-β1, and IL-8 were reported as total amount
421 (pg) contained in the entire volume of apical (100 μl) and basolateral (600 μl) culture supernatants.
422
423 **Statistical analysis**
424 Statistical significances were calculated using the Student's *t*-test unpaired, one-way or two-way
425 analysis of variance (ANOVA) with Tukey's post-test as appropriate, using Prism software v7.02

(GraphPad, San Diego, CA). Treatment comparisons included at least three replicates and three independent experiments. Differences were considered statistically significant at p-value ≤ 0.05. Exact p values are indicated in each Figure. Results are expressed as mean $\pm$ standard error of mean (sem).

Acknowledgements

The authors want to thank Dr. Mark Donowitz, for critical reading of the manuscript and Robin Barnes and Nancy Greenberg, Clinical Research Nurses at University of Maryland, for their assistance in obtaining peripheral blood samples. The authors would like to acknowledge the Integrated Physiology Core of the Hopkins Conte Digestive Disease Basic and Translational Research Core Center (NIH P30 DK-089502 to N.C.Z.) for providing human enteroids and growth factor conditioned media and the University of Maryland School of Medicine Center for Innovative Biomedical Resources, Flow Cytometry Shared Service. This work was supported by NIH/NIAID P01AI125181 Immunology and Enteroid Cores, and 1R01AI117734-01 to M.F.P.

Author Contributions

J.M.L-D. designed and performed experiments, conducted data analyses and interpretation. M.D. provided initial assistance with enteroid monolayers. N.C.Z. and M.F.P. participated in experimental design, data analyses and interpretation, and supervised the study. J.M.L-D. and M.F.P. wrote the manuscript. All authors edited the manuscript.

Disclosures

The authors have no financial conflicts of interest.

References

1. Peterson, L. W. & Artis, D. Intestinal epithelial cells: regulators of barrier function and immune homeostasis. *Nat. Rev. Immunol.* **14**, 141-153 (2014).
2. Mestas, J. & Hughes, C. C. Of mice and not men: differences between mouse and human immunology. *J. Immunol.* **172**, 2731-2738 (2004).
3. Gibbons, D. L. & Spencer, J. Mouse and human intestinal immunity: same ballpark, different players; different rules, same score. *Mucosal Immunol.* **4**, 148-157 (2011).
4. Barker, N., van Es, J. H., Kuipers, J., Kujala, P., van den Born, M., Cozijnsen, M. *et al.* Identification of stem cells in small intestine and colon by marker gene Lgr5. *Nature* **449**, 1003-1007 (2007).
5. Zhang, Y. G., Wu, S., Xia, Y. & Sun, J. Salmonella-infected crypt-derived intestinal organoid culture system for host-bacterial interactions. *Physiol. Rep.* **2**, e12147 (2014).
6. Huang, J. Y., Sweeney, E. G., Sigal, M., Zhang, H. C., Remington, S. J., Cantrell, M. A. *et al.* Chemodetection and destruction of host urea allows Helicobacter pylori to locate the epithelium. *Cell Host Microbe* **18**, 147-156 (2015).
7. Co, J. Y., Margalef-Catala, M., Li, X., Mah, A. T., Kuo, C. J., Monack, D. M. *et al.* Controlling epithelial polarity: A human enteroid model for host-pathogen interactions. *Cell Rep.* **26**, 2509-2520.e2504 (2019).
8. Foulke-Abel, J., In, J., Kovbasnjuk, O., Zachos, N. C., Ettayebi, K., Blutt, S. E. *et al.* Human enteroids as an ex-vivo model of host-pathogen interactions in the gastrointestinal tract. *Exp. Biol. Med. (Maywood)* **239**, 1124-1134 (2014).
9. In, J., Foulke-Abel, J., Zachos, N. C., Hansen, A. M., Kaper, J. B., Bernstein, H. D. *et al.* Enterohemorrhagic Escherichia coli reduce mucus and intermicrovillar bridges in human stem cell-derived colonoids. *Cell. Mol. Gastroenterol. Hepatol.* **2**, 48-62 e43 (2016).
10. Rajan, A., Vela, L., Zeng, X. L., Yu, X., Shroyer, N., Blutt, S. E. *et al.* Novel segment- and host-specific patterns of Enteroaggregative Escherichia coli adherence to human intestinal enteroids. *mBio.* **9**, e02419-02417 (2018).
11. In, J. G., Foulke-Abel, J., Estes, M. K., Zachos, N. C., Kovbasnjuk, O. & Donowitz, M. Human mini-guts: new insights into intestinal physiology and host-pathogen interactions. *Nat. Rev. Gastroenterol. Hepatol.* **13**, 633-642 (2016).
12. Noel, G., Baetz, N. W., Staab, J. F., Donowitz, M., Kovbasnjuk, O., Pasetti, M. F. *et al.* A primary human macrophage-enteroid co-culture model to investigate mucosal gut physiology and host-pathogen interactions. *Sci. Rep.* **7**, 45270 (2017).
13. Noel, G., Doucet, M., Nataro, J. P., Kaper, J. B., Zachos, N. C. & Pasetti, M. F. Enterotoxigenic Escherichia coli is phagocytosed by macrophages underlying villus-like intestinal epithelial cells: modeling ex vivo innate immune defenses of the human gut. *Gut Microbes* **9**, 382-389 (2018).
14. Sansonetti, P. J., Arondel, J., Cantey, J. R., Prevost, M. C. & Huerre, M. Infection of rabbit Peyer's patches by Shigella flexneri: effect of adhesive or invasive bacterial phenotypes on follicle-associated epithelium. *Infect. Immun.* **64**, 2752-2764 (1996).
15. Gustafson, M. P., Lin, Y., Maas, M. L., Van Keulen, V. P., Johnston, P. B., Peikert, T. *et al.* A method for identification and analysis of non-overlapping myeloid immunophenotypes in humans. *PLoS One* **10**, e0121546 (2015).

16. Metzemaekers, M., Vandendriessche, S., Berghmans, N., Gouwy, M. & Proost, P. Truncation of CXCL8 to CXCL8(9-77) enhances actin polymerization and in vivo migration of neutrophils. *J. Leukoc. Biol.* **107**, 1167-1173 (2020).
17. Fournier, B. M. & Parkos, C. A. The role of neutrophils during intestinal inflammation. *Mucosal Immunol.* **5**, 354-366 (2012).
18. Lekstrom-Himes, J. A. & Gallin, J. I. Immunodeficiency diseases caused by defects in phagocytes. *N. Engl. J. Med.* **343**, 1703-1714 (2000).
19. Wortmann, S. B., Van Hove, J. L. K., Derks, T. G. J., Chevalier, N., Knight, V., Koller, A. *et al.* Treating neutropenia and neutrophil dysfunction in glycogen storage disease IB with an SGLT2-inhibitor. *Blood*, 2019004465 (2020).
20. Blikslager, A. T., Moeser, A. J., Gookin, J. L., Jones, S. L. & Odle, J. Restoration of barrier function in injured intestinal mucosa. *Physiol. Rev.* **87**, 545-564 (2007).
21. Sullivan, D. P., Bui, T., Muller, W. A., Butin-Israeli, V. & Sumagin, R. In vivo imaging reveals unique neutrophil transendothelial migration patterns in inflamed intestines. *Mucosal Immunol.* **11**, 1571-1581 (2018).
22. Lammermann, T., Afonso, P. V., Angermann, B. R., Wang, J. M., Kastenmuller, W., Parent, C. A. *et al.* Neutrophil swarms require LTB4 and integrins at sites of cell death in vivo. *Nature* **498**, 371-375 (2013).
23. Uderhardt, S., Martins, A. J., Tsang, J. S., Lammermann, T. & Germain, R. N. Resident macrophages cloak tissue microlesions to prevent neutrophil-driven inflammatory damage. *Cell* **177**, 541-555 e517 (2019).
24. Sumagin, R., Robin, A. Z., Nusrat, A. & Parkos, C. A. Transmigrated neutrophils in the intestinal lumen engage ICAM-1 to regulate the epithelial barrier and neutrophil recruitment. *Mucosal Immunol.* **7**, 905-915 (2014).
25. Parkos, C. A., Delp, C., Arnaout, M. A. & Madara, J. L. Neutrophil migration across a cultured intestinal epithelium. Dependence on a CD11b/CD18-mediated event and enhanced efficiency in physiological direction. *J. Clin. Invest.* **88**, 1605-1612 (1991).
26. Brazil, J. C., Liu, R., Sumagin, R., Kolegraff, K. N., Nusrat, A., Cummings, R. D. *et al.* alpha3/4 Fucosyltransferase 3-dependent synthesis of Sialyl Lewis A on CD44 variant containing exon 6 mediates polymorphonuclear leukocyte detachment from intestinal epithelium during transepithelial migration. *J. Immunol.* **191**, 4804-4817 (2013).
27. Flemming, S., Luissint, A. C., Nusrat, A. & Parkos, C. A. Analysis of leukocyte transepithelial migration using an in vivo murine colonic loop model. *JCI Insight* **3**, e99722 (2018).
28. Masoodi, I., Kochhar, R., Dutta, U., Vaishnavi, C., Prasad, K. K., Vaiphei, K. *et al.* Evaluation of fecal myeloperoxidase as a biomarker of disease activity and severity in ulcerative colitis. *Dig. Dis. Sci.* **57**, 1336-1340 (2012).
29. Kolaczkowska, E. & Kubes, P. Neutrophil recruitment and function in health and inflammation. *Nat. Rev. Immunol.* **13**, 159-175 (2013).
30. Grunwell, J. R., Giacalone, V. D., Stephenson, S., Margaroli, C., Dobosh, B. S., Brown, M. R. *et al.* Neutrophil dysfunction in the airways of children with acute respiratory failure due to lower respiratory tract viral and bacterial coinfections. *Sci. Rep.* **9**, 2874 (2019).
31. Svedberg, F. R., Brown, S. L., Krauss, M. Z., Campbell, L., Sharpe, C., Clausen, M. *et al.* The lung environment controls alveolar macrophage metabolism and responsiveness in type 2 inflammation. *Nat. Immunol.* **20**, 571-580 (2019).

32. Vainer, B., Nielsen, O. H. & Horn, T. Comparative studies of the colonic in situ expression of intercellular adhesion molecules (ICAM-1, -2, and -3), beta2 integrins (LFA-1, Mac-1, and p150,95), and PECAM-1 in ulcerative colitis and Crohn's disease. *Am. J. Surg. Pathol.* **24**, 1115-1124 (2000).
33. Liu, Y., Merlin, D., Burst, S. L., Pochet, M., Madara, J. L. & Parkos, C. A. The role of CD47 in neutrophil transmigration. Increased rate of migration correlates with increased cell surface expression of CD47. *J. Biol. Chem.* **276**, 40156-40166 (2001).
34. Parkos, C. A., Colgan, S. P., Liang, T. W., Nusrat, A., Bacarra, A. E., Carnes, D. K. *et al.* CD47 mediates post-adhesive events required for neutrophil migration across polarized intestinal epithelia. *J. Cell. Biol.* **132**, 437-450 (1996).
35. Golay, J., Valgardsdottir, R., Musaraj, G., Giupponi, D., Spinelli, O. & Introna, M. Human neutrophils express low levels of FcgammaRIIIA, which plays a role in PMN activation. *Blood* **133**, 1395-1405 (2019).
36. Teschner, D., Cholaszczynska, A., Ries, F., Beckert, H., Theobald, M., Grabbe, S. *et al.* CD11b regulates fungal outgrowth but not neutrophil recruitment in a mouse model of invasive pulmonary aspergillosis. *Front. Immunol.* **10**, 123 (2019).
37. Altstaedt, J., Kirchner, H. & Rink, L. Cytokine production of neutrophils is limited to interleukin-8. *Immunology* **89**, 563-568 (1996).
38. Andrews, C., McLean, M. H. & Durum, S. K. Cytokine tuning of intestinal epithelial function. *Front. Immunol.* **9**, 1270 (2018).
39. Ruder, B., Atreya, R. & Becker, C. Tumour necrosis factor alpha in intestinal homeostasis and gut related diseases. *Int. J. Mol. Sci.* **20**, (2019).
40. Ranganathan, S., Doucet, M., Grassel, C. L., Delaine-Elias, B., Zachos, N. C. & Barry, E. M. Evaluating Shigella flexneri pathogenesis in the human enteroid model. *Infect. Immun.* **87**, e00740-00718 (2019).
41. Koestler, B. J., Ward, C. M., Fisher, C. R., Rajan, A., Maresso, A. W. & Payne, S. M. Human intestinal enteroids as a model system of Shigella pathogenesis. *Infect. Immun.* **87**, e00733-00718 (2019).
42. Kotloff, K. L., Riddle, M. S., Platts-Mills, J. A., Pavlinac, P. & Zaidi, A. K. M. Shigellosis. *Lancet* **391**, 801-812 (2018).
43. Perdomo, O. J., Cavaillon, J. M., Huerre, M., Ohayon, H., Gounon, P. & Sansonetti, P. J. Acute inflammation causes epithelial invasion and mucosal destruction in experimental shigellosis. *J. Exp. Med.* **180**, 1307-1319 (1994).
44. Perdomo, J. J., Gounon, P. & Sansonetti, P. J. Polymorphonuclear leukocyte transmigration promotes invasion of colonic epithelial monolayer by Shigella flexneri. *J. Clin. Invest.* **93**, 633-643 (1994).
45. Coron, E., Flamant, M., Aubert, P., Wedel, T., Pedron, T., Letessier, E. *et al.* Characterisation of early mucosal and neuronal lesions following Shigella flexneri infection in human colon. *PLoS One* **4**, e4713 (2009).
46. Kuhn, K. A., Manieri, N. A., Liu, T. C. & Stappenbeck, T. S. IL-6 stimulates intestinal epithelial proliferation and repair after injury. *PLoS One* **9**, e114195 (2014).
47. Ye, D., Ma, I. & Ma, T. Y. Molecular mechanism of tumor necrosis factor-alpha modulation of intestinal epithelial tight junction barrier. *Am. J. Physiol. Gastrointest. Liver Physiol.* **290**, G496-504 (2006).

48. Sellge, G., Magalhaes, J. G., Konradt, C., Fritz, J. H., Salgado-Pabon, W., Eberl, G. *et al.* Th17 cells are the dominant T cell subtype primed by Shigella flexneri mediating protective immunity. *J. Immunol.* **184**, 2076-2085 (2010).
49. Lindberg, F. P., Bullard, D. C., Caver, T. E., Gresham, H. D., Beaudet, A. L. & Brown, E. J. Decreased resistance to bacterial infection and granulocyte defects in IAP-deficient mice. *Science* **274**, 795-798 (1996).
50. Azcutia, V., Kelm, M., Luissint, A. C., Boerner, K., Flemming, S., Quiros, M. *et al.* Neutrophil expressed CD47 regulates CD11b/CD18-dependent neutrophil transepithelial migration in the intestine in vivo. *Mucosal Immunol.*, (2020).
51. Jaiswal, S., Jamieson, C. H., Pang, W. W., Park, C. Y., Chao, M. P., Majeti, R. *et al.* CD47 is upregulated on circulating hematopoietic stem cells and leukemia cells to avoid phagocytosis. *Cell* **138**, 271-285 (2009).
52. Zhang, Z., Jin, L., Champion, G., Seydel, K. B. & Stanley, S. L., Jr. Shigella infection in a SCID mouse-human intestinal xenograft model: role for neutrophils in containing bacterial dissemination in human intestine. *Infect. Immun.* **69**, 3240-3247 (2001).
53. Trevani, A. S., Andonegui, G., Giordano, M., Lopez, D. H., Gamberale, R., Minucci, F. *et al.* Extracellular acidification induces human neutrophil activation. *J. Immunol.* **162**, 4849-4857 (1999).
54. Sato, T., Stange, D. E., Ferrante, M., Vries, R. G., Van Es, J. H., Van den Brink, S. *et al.* Long-term expansion of epithelial organoids from human colon, adenoma, adenocarcinoma, and Barrett's epithelium. *Gastroenterology* **141**, 1762-1772 (2011).
55. In, J. G., Foulke-Abel, J., Clarke, E. & Kovbasnjuk, O. Human colonoid monolayers to study interactions between pathogens, commensals, and host intestinal epithelium. *J. Vis. Exp.*, (2019).
56. Parkos, C. A., Colgan, S. P., Delp, C., Arnaout, M. A. & Madara, J. L. Neutrophil migration across a cultured epithelial monolayer elicits a biphasic resistance response representing sequential effects on transcellular and paracellular pathways. *J. Cell. Biol.* **117**, 757-764 (1992).
57. Brouwer, N., Dolman, K. M., van Houdt, M., Sta, M., Roos, D. & Kuijpers, T. W. Mannose-binding lectin (MBL) facilitates opsonophagocytosis of yeasts but not of bacteria despite MBL binding. *J. Immunol.* **180**, 4124-4132 (2008).
58. Chaka, W., Scharringa, J., Verheul, A. F., Verhoef, J., Van Strijp, A. G. & Hoepelman, I. M. Quantitative analysis of phagocytosis and killing of Cryptococcus neoformans by human peripheral blood mononuclear cells by flow cytometry. *Clin. Diagn. Lab. Immunol.* **2**, 753-759 (1995).

Figure legends

Figure 1. Establishment of a human PMN-enteroid co-culture. (**a**) Process of PMN isolation from peripheral blood and May-Grünwald Giemsa image [left]. Representative dot plot of PMN phenotype [middle] and schematic representation PMN-enteroid co-culture model [right]. (**b**) Confocal XZ projection [top; right, magnification XY projection] and H&E [bottom] images of the PMN-enteroid co-culture. Confocal: DNA, blue; actin, white; CD16 (PMN), green; Transwell insert, dashed lines. Arrowheads indicate PMN seeded on the Transwell insert and at the base of the columnar epithelium. (**c**) Representative immunofluorescence confocal microscopy image [top, XY; bottom, XZ projections] showing transmigrating PMN within the epithelial cell monolayer. DNA, blue; CD16 (PMN), green; actin, white; Transwell insert, dashed line. (**d**) Number of PMN transmigrated to the apical compartment after 2h of incubation with enteroid monolayers. (**e**) TER of PMN-enteroid co-cultures at 2h. (**f**) Total amount of cytokines secreted into the apical and basolateral compartments after 2h of co-culture. (**g**) Numbers of PMN transmigrated to luminal compartment 2h after of apical treatment with rhIL-8. Blue shadow denotes mean ± sem of data shown in (d); *p* value comparing (d) vs. (g). (**h**) TER of enteroid monolayers and PMN-enteroid co-culture apically treated with rhIL-8 for 2h. (d,e,g,h) Each dot represents the average from three replicate wells; data are shown as mean ± sem from 3 independent experiments. (f) Data are shown as mean + sem from 3 independent experiments in triplicate. *p* values were calculated by Student's *t* test.

Figure 2. Distinctive PMN phenotype in the human intestinal environment. (**a**) Schematic representation of PMN in direct contact with epithelial cells (C) or in the basolateral media (BM). (**b, c, d**) Phenotype of freshly isolated PMN, PMN in C and BM determined by flow cytometry within 2h of co-culture. Each dot represents data collected from three replicate wells; data are shown as mean ± sem from 3 independent experiments. *p* values were calculated by one-way-ANOVA with Tukey's post-test for multiple comparisons.

Figure 3. Innate immune responses of human PMN to *S. flexneri*. (**a**) Representative confocal microscopy image and histogram of *S. flexneri* 2a-FITC uptake by human PMN. Confocal image [left, XY projection]. DNA, blue; actin, red; *S. flexneri 2a*, green. Histograms of PMN harboring *Shigella*-FITC [middle] and percentage of phagocytosis at 10, 30 and 60 min post infection [left]. Each dot represents the average from three replicates and PMN from 5 individual donors; data are shown as mean ± sem from 3 independent experiments. (**b**) Extracellular *S. flexneri* 2a colony forming units (CFU) in PMN culture media at 10, 30 and 60 min post infection. Each dot represents the average from three replicates and PMN from 6 individual donors; data are shown as mean ± sem from 3 independent experiments. (a, b) *p* values were calculated by one-way ANOVA with Tukey's post-test for multiple comparisons. (**c**) PMN viability in the presence and absence of *S. flexneri* 2a. Data represents the average from three replicates and PMN from 3 individual donors; data are shown as mean ± sem from 3 independent experiments. (**d**) PMN morphology before (0 min) and after (30 min) exposure to *S. flexneri* 2a. (**e**) Confocal microscopy image [XY projection] of NET 30 min after exposure to *S. flexneri* 2a. DNA, blue; actin, red; *S. flexneri* 2a, green. (**f**) Immunofluorescence image showing *S. flexneri* 2a-FITC colocalization in PMN lysosome. Arrowheads indicate bacteria intracellularly and within the lysosome compartment. (**g**) Total amount of cytokines secreted into the culture media of PMN alone and PMN exposed to *S. flexneri* 2a for 2h. Data are shown as mean ± sem from 3 independent experiments in triplicate. (c, g) *p* values were calculated by Student's *t* test.

Figure 4. *Shigella* infection of PMN-enteroid co-cultures. (**a**) Numbers of PMN transmigrated to the apical compartment of enteroid monolayers exposed or not to *S. flexneri* 2a for 2h. (**b**) Confocal microscopy images [top, XY; bottom, XZ projections; right, magnification] of PMN-enteroid co-culture infected with *S. flexneri* 2a for 2h. CD16 (PMN), green; *S. flexneri* 2a, red; actin, white. Arrowheads indicate *S. flexneri* 2a. (**c**) CFU in the apical and basolateral media of

enteroid and PMN-enteroid co-cultures apically exposed to *S. flexneri* 2a for 2h. (**d**) TER of enteroid and PMN-enteroid co-cultures exposed to *S. flexneri* 2a for 2h. (**e**) Total amount of cytokines in the apical and basolateral media of PMN-enteroid co-cultures exposed or not to *S. flexneri* 2a for 2h. (a,c,d) Each dot represents the average from three replicate wells; data are shown as mean ± sem from 3 (a, d) and 5 (c) independent experiments. *p* values were calculated by Student's *t* test. (e) Data are shown as mean + sem from 3 independent experiments in triplicate. *p* values were calculated by Student's *t* test.

Figure 5. Immune phenotype of PMN co-cultured with epithelial cells and exposed to *Shigella*. (**a, b, c**) Cell surface expression of CD15, CD16, CD11b, CD18, CD88, CD66b, CD47, and CD182 on PMN in the enteroid co-culture exposed or not to *S. flexneri* 2a for 2h. Each dot represents data collected from three replicate wells; data are shown as mean ± sem from 3 independent experiments. *p* values were calculated by Student's *t* test.

Figure 1.

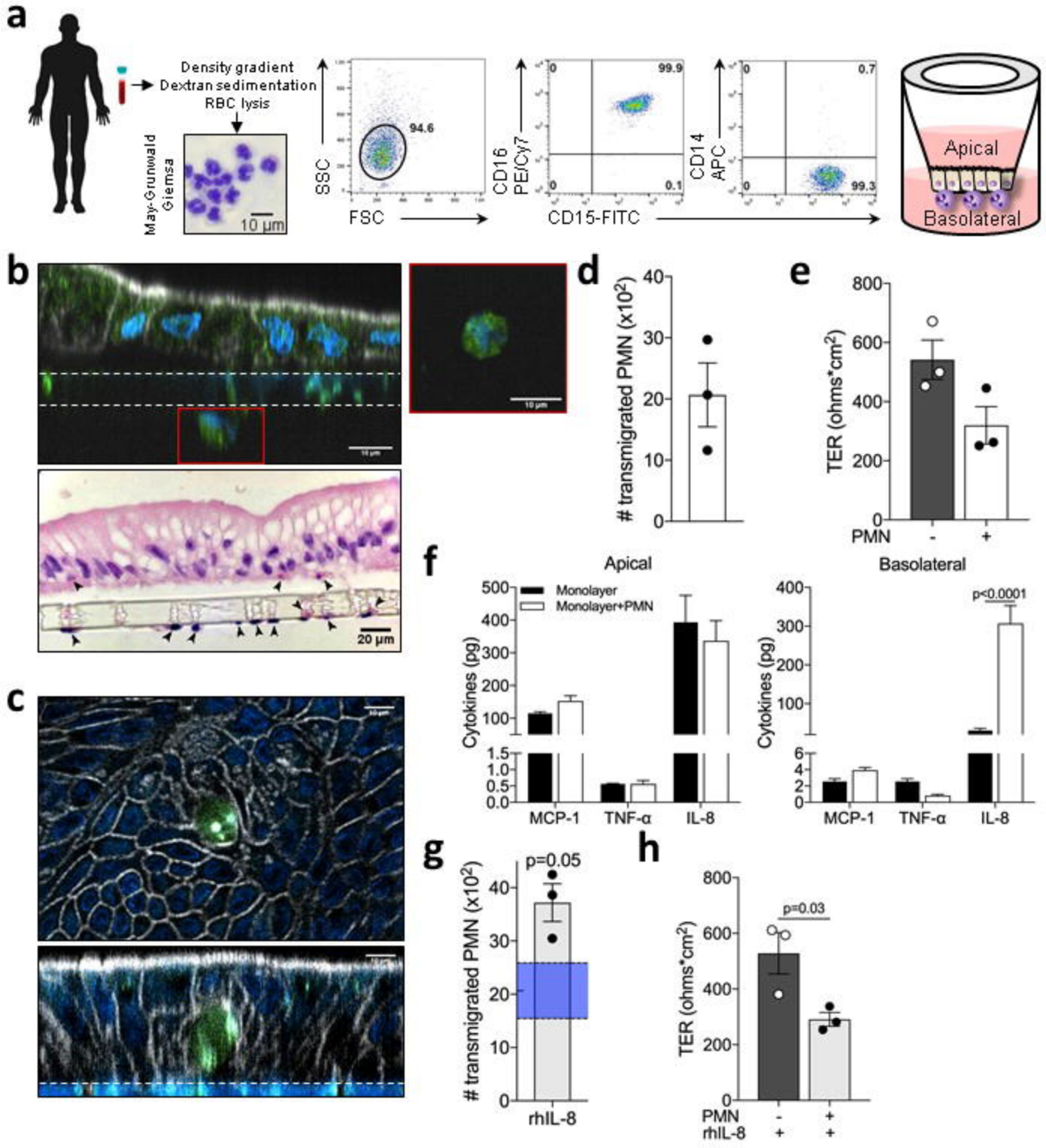
a
Density gradient
Dextran sedimentation
RBC lysis
May-Grunwald Giemsa
10 µm
SSC
FSC
94.6
CD16 PE/Cy7
CD15-FITC
99.9
0.1
CD14 APC
0.7
99.3
Apical
Basolateral
b
20 µm
c
d
transmigrated PMN (x10²)
e
TER (ohms*cm²)
PMN
f
Apical
Basolateral
Monolayer
Monolayer+PMN
Cytokines (pg)
MCP-1
TNF-α
IL-8
p<0.0001
g
p=0.05
# transmigrated PMN (x10²)
rhIL-8
h
p=0.03
TER (ohms*cm²)
PMN
rhIL-8

Figure 2.

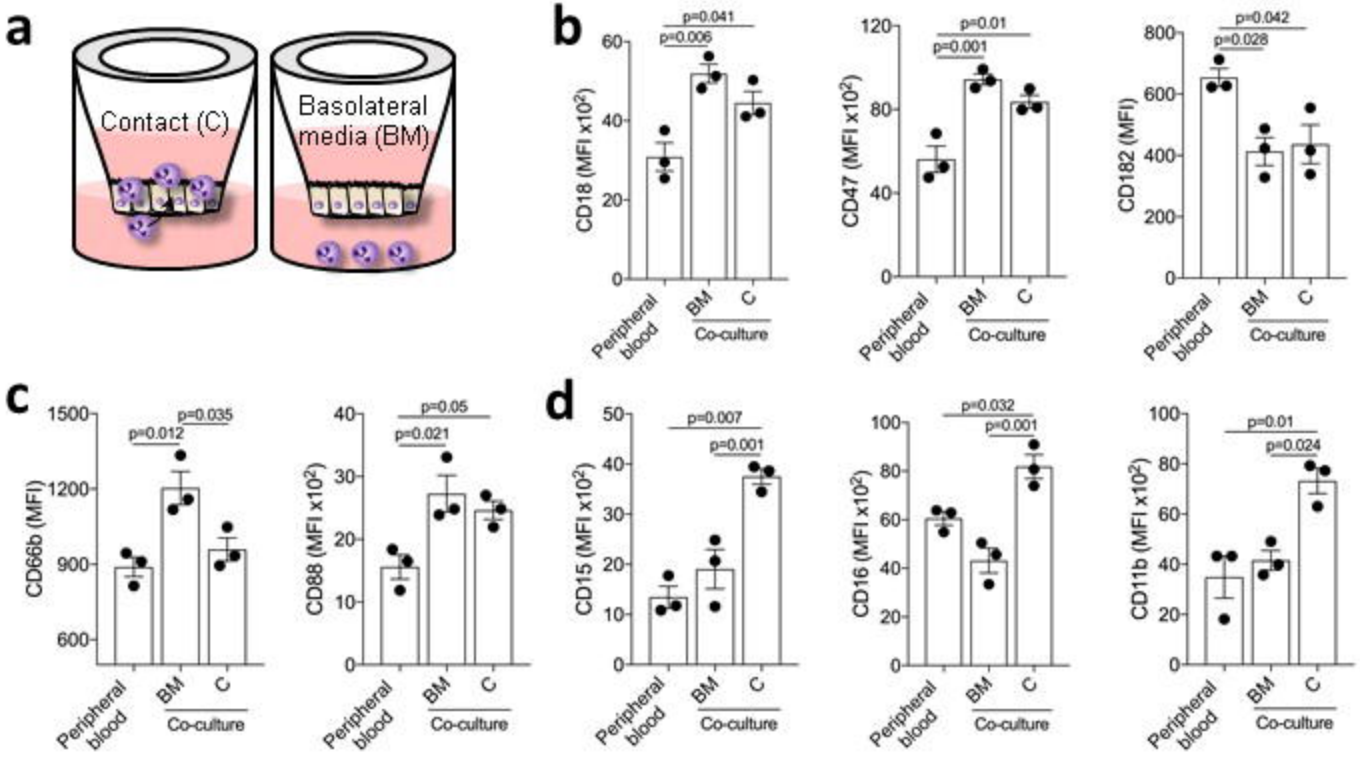
a
Contact (C)
Basolateral media (BM)
b
CD18 (MFI x10²)
p=0.041
p=0.006
CD47 (MFI x10²)
p=0.01
p=0.001
CD182 (MFI)
p=0.042
p=0.028
Peripheral blood
BM
C
Co-culture
c
CD66b (MFI)
p=0.035
p=0.012
CD88 (MFI x10²)
p=0.05
p=0.021
d
CD15 (MFI x10²)
p=0.007
p=0.001
CD16 (MFI x10²)
p=0.032
p=0.001
CD11b (MFI x10²)
p=0.01
p=0.024

Figure 3.

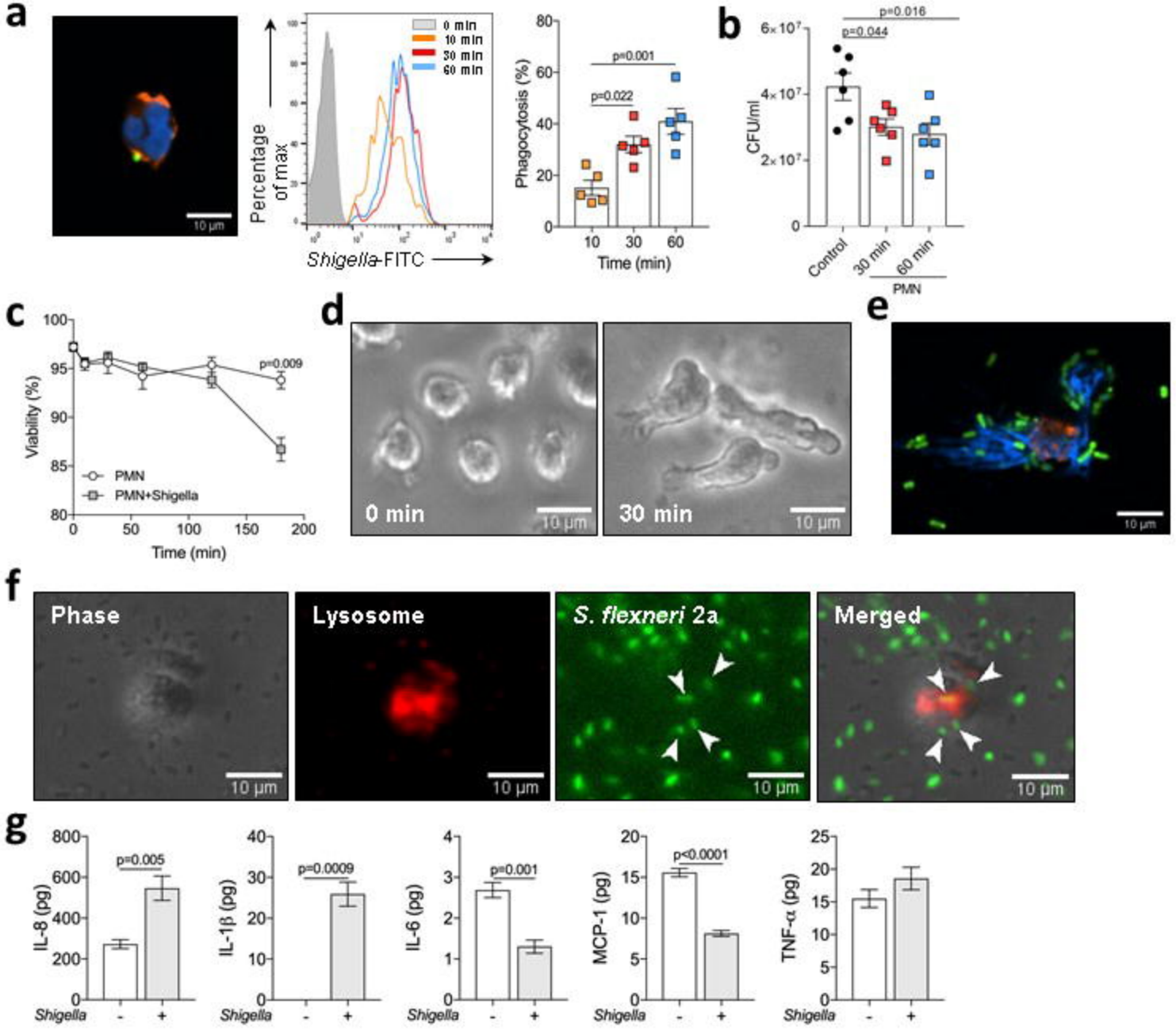
a
10 μm
Percentage of max
Shigella-FITC
0 min
10 min
30 min
60 min
Phagocytosis (%)
p=0.001
p=0.022
Time (min)
b
CFU/ml
p=0.016
p=0.044
Control
30 min
60 min
PMN
c
Viability (%)
p=0.009
PMN
PMN+Shigella
Time (min)
d
0 min
30 min
10 μm
e
f
Phase
Lysosome
S. flexneri 2a
Merged
g
IL-8 (pg)
p=0.005
IL-1β (pg)
p=0.0009
IL-6 (pg)
p=0.001
MCP-1 (pg)
p<0.0001
TNF-α (pg)
Shigella

Figure 4.

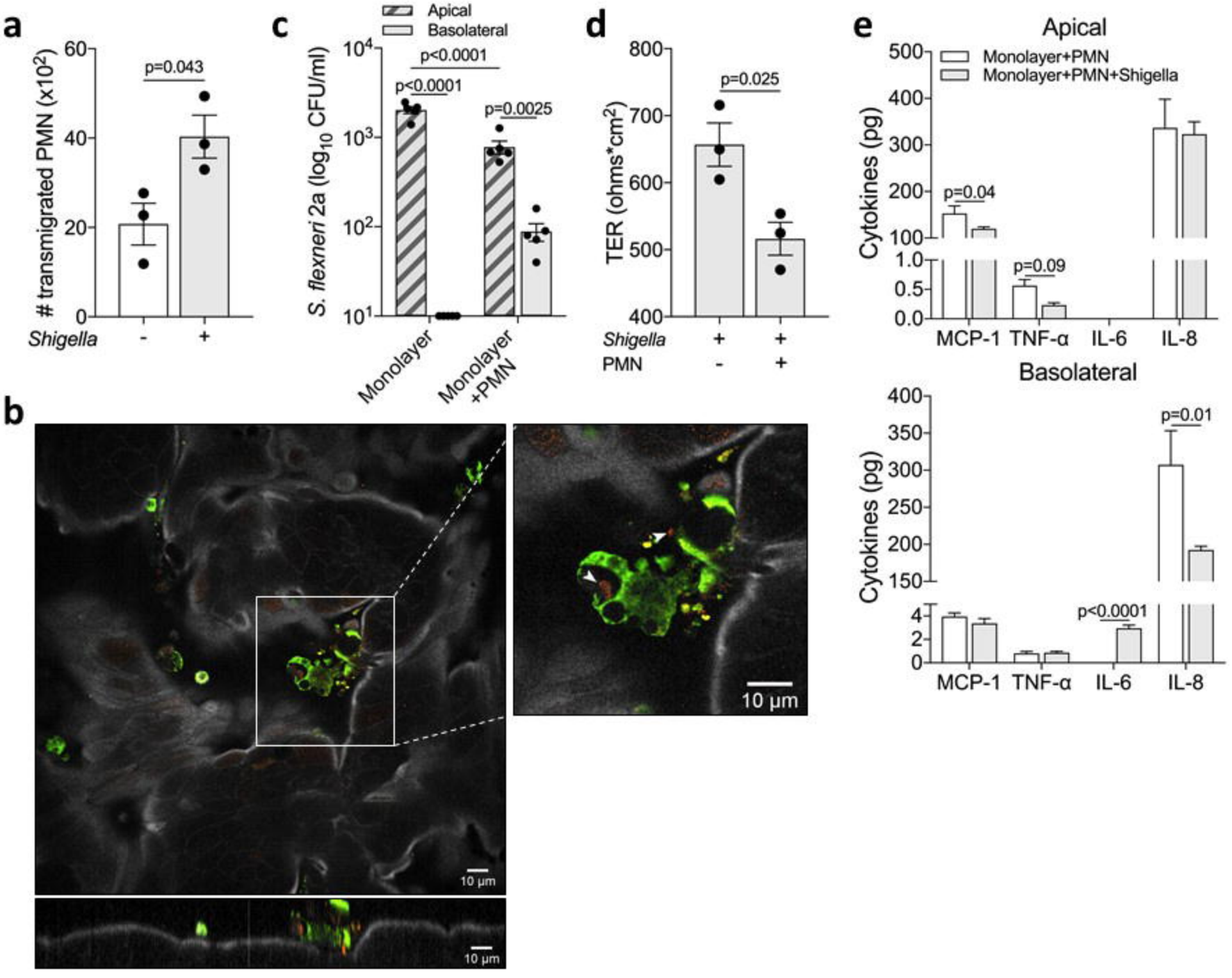
a
# transmigrated PMN (x10²)
p=0.043
Shigella
c
Apical
Basolateral
S. flexneri 2a (log10 CFU/ml)
p<0.0001
p<0.0001
p=0.0025
Monolayer
Monolayer +PMN
d
TER (ohms*cm²)
p=0.025
Shigella
PMN
e
Apical
Monolayer+PMN
Monolayer+PMN+Shigella
Cytokines (pg)
p=0.04
p=0.09
MCP-1
TNF-α
IL-6
IL-8
Basolateral
p=0.01
p<0.0001
b
10 µm
10 µm
10 µm

Figure 5.

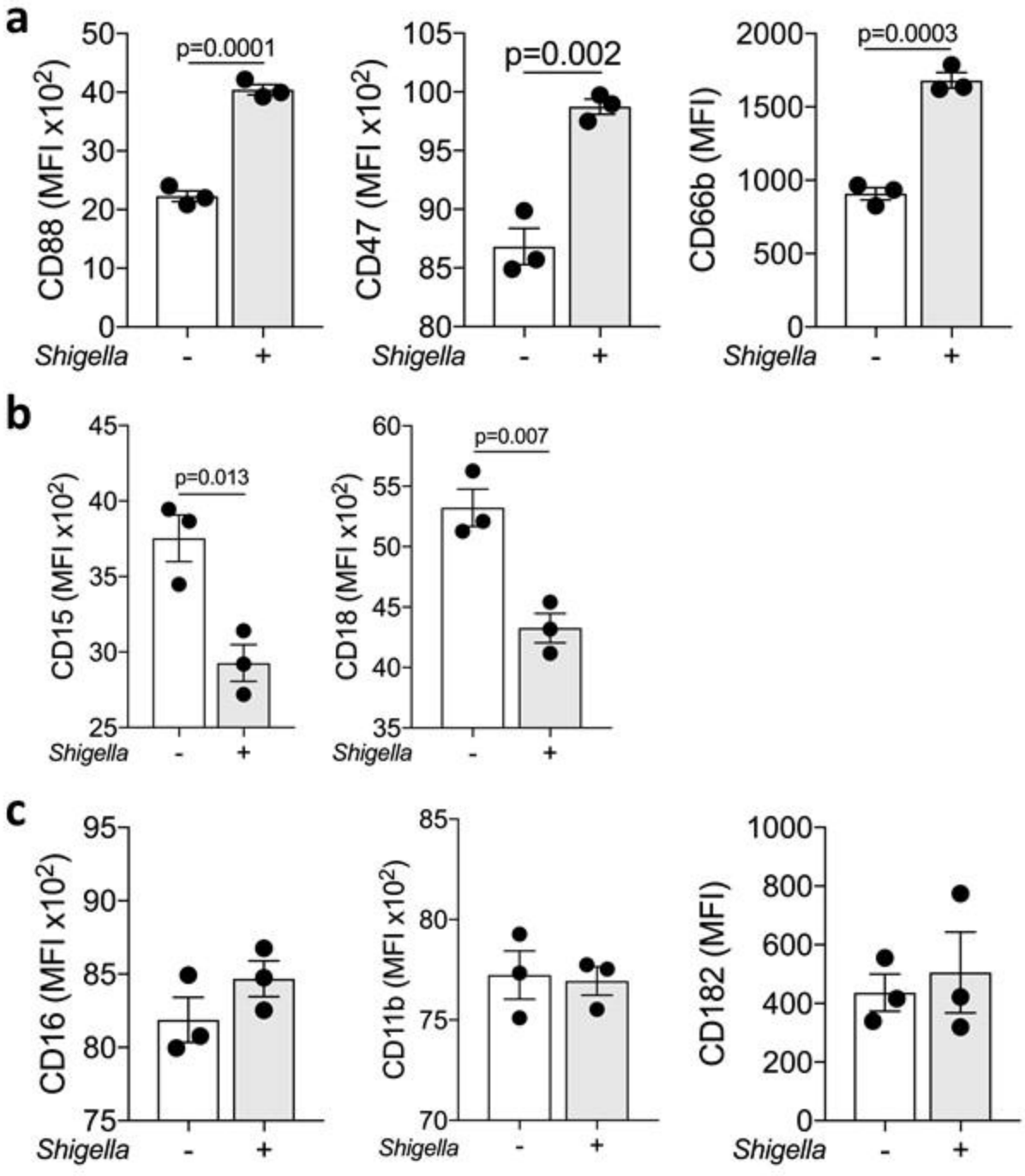
a
CD88 (MFI x10²)
p=0.0001
Shigella - +
CD47 (MFI x10²)
p=0.002
Shigella - +
CD66b (MFI)
p=0.0003
Shigella - +
b
CD15 (MFI x10²)
p=0.013
Shigella - +
CD18 (MFI x10²)
p=0.007
Shigella - +
c
CD16 (MFI x10²)
Shigella - +
CD11b (MFI x10²)
Shigella - +
CD182 (MFI)
Shigella - +